Mem. Natl Inst. Polar Res., Spec. Issue, **55**, 105–126, 2001

Petrography and mineral chemistry of high-grade pelitic gneisses and related rocks from Namaqualand, South Africa

Tomokazu Hokada[1,*], Yoichi Motoyoshi[1], Yoshikuni Hiroi[2], Toshiaki Shimura[3], Masaki Yuhara[4], Kazuyuki Shiraishi[1], Geoffrey H. Grantham[5] and Mike W. Knoper[6]

[1]*National Institute of Polar Research, Kaga 1-chome, Itabashi-ku, Tokyo 173-8515*
[2]*Department of Earth Sciences, Faculty of Science, Chiba University, 1-33, Yayoi-cho, Chiba 263-8522*
[3]*Department of Geology, Faculty of Science, Niigata University, 2-8050, Ikarashi, Niigata 950-2181*
[4]*Department of Earth System Science, Faculty of Science, Fukuoka University, 19-1, Nanakuma 8-chome, Jonan-ku, Fukuoka 814-0180*
[5]*Council for Geoscience, P/Bag X112, Silverton 0127, South Africa*
[6]*Department of Geology, Rand Afrikaans University, PO Box 524, Auckland Park 2006, South Africa*

Abstract: Four different types of paragneisses, (1) ordinary pelitic gneiss, (2) sapphirine-bearing aluminous gneiss, (3) osumilite-bearing magnesian gneiss, and (4) quartz-magnetite-rich ferruginous gneiss, occur in the Namaqualand Metamorphic Complex in South Africa. They are examined with respect to their mineral parageneses and mineral chemistries for assessing chemical evolution during high temperature metamorphism. (1) Ordinary pelitic gneisses show amphibolite to granulite facies mineral parageneses composed of biotite, sillimanite, cordierite, garnet and spinel with or without orthopyroxene. Other rock types (2) ~ (4), occurring as layers or blocks in pelitic gneiss, granitic orthogneiss or mafic granulite, show characteristic mineral parageneses: (2) Aluminous gneiss is characterized by quartz-free silica-undersaturated mineral parageneses, and contains porphyroblastic clots of sapphirine-spinel-corundum aggregate. (3) Osumilite-bearing magnesian gneiss is composed mainly of quartz, plagioclase, cordierite and osumilite which is mostly replaced by a fine-grained symplectite of cordierite-K-feldspar-quartz-orthopyroxene. Biotite, spinel and orthopyroxene are minor. (4) Ferruginous gneiss contains a large volume of magnetite accompanying quartz, sillimanite and spinel. Feldspar is typically lacking.

Biotite in paragneisses contains a varying amount of fluorine, up to 5.8 wt%, having no systematic relation to whether it coexists with orthopyroxene or not. Geothermobarometries for coexisting garnet and orthopyroxene yield metamorphic conditions around 850℃ and 0.5 GPa. Orthopyroxene contains high Al_2O_3, up to 8.5 wt%, and is probably formed by the dehydration melting of biotite at the peak of metamorphism. ZnO contents of spinel in pelitic, ferruginous and magnesian gneisses range from 0.3 to 13.7 wt%, whereas those in the sapphirine-bearing aluminous gneisses are less than 0.5 wt%.

key words: granulite, high temperature metamorphism, Namaqualand, paragneiss, pelitic gneiss

*Present address: Department of Geology, National Science Museum, 3-23-1, Hyakunin-cho, Shinjuku-ku, Tokyo 169-0073 (hokada@kahaku.go.jp).

1. Introduction

Granulite facies metamorphic rocks are considered to be one of the major components of the mid to lower part of the continental crust. The amphibolite-granulite facies transition is defined by the first appearance of orthopyroxene as substitute for amphibole (or biotite) in mafic rocks (*e.g.*, Spear, 1993). Orthopyroxene is also generated in a slightly higher-grade zone of granulite facies in pelitic rocks, possibly through dehydration melting of biotite. Partial melting should cause chemical differentiation and also change the physical properties of rocks. Therefore, the amphibolite-granulite-transition is a major chemical and rheological boundary in the continental crust, and, thus, the formation of the granulite-facies rocks from amphibolite-facies rocks directly manifests the deep crustal process.

The Namaqualand Metamorphic Complex in South Africa has attracted petrological interest as the occurrence of the high-temperature mineral parageneses including biotite, sillimanite, cordierite, garnet, spinel, orthopyroxene, sapphirine and osumilite in metapelitic rocks. Petrological and geochronological studies have indicated that the amphibolite to granulite facies metamorphism (~870°C) occurred at relatively shallower crustal levels (0.4–0.6 GPa) during the multiple thermal events at 1220–1170 Ma and 1060–1030 Ma (Waters, 1989; Clifford *et al.*, 1995; Robb *et al.*, 1999). Robb *et al.* (1999) suggested that compressional heating to granulite facies conditions followed by isobaric cooling, say along an anticlockwise *P-T* path, in Namaqualand resulted from crustal thickening and subsequent magmatic accretion at 1060–1030 Ma.

Granulite facies metamorphism in Namaqualand is well documented by detailed petrological studies, such as partial melting of metapelites (Waters and Whales, 1984; Waters, 1988), petrology of sapphirine-bearing paragenesis (Waters, 1986), that of boro-silicates (Waters and Moore, 1985; Moore *et al.*, 1990), spinel-quartz paragenesis (Waters, 1991), osumilite-bearing paragenesis (Nowicki *et al.*, 1995), and the relationship between metamorphism and deformation (Raith and Harley, 1998). Hiroi *et al.* (2001, this volume) provides new evidence for prograde metamorphism and partial melting of Mg-Al-rich rocks in the same area. Nevertheless, uncertainty remains with respect to the modes of occurrence of orthopyroxene and the chemical features of coexisting minerals. From this perspective, here we present new petrographical and mineralogical data on pelitic gneisses and related rocks from the high-grade region of the Namaqualand Metamorphic Complex, and give a brief discussion.

2. Geological setting and sample localities

The Namaqualand Metamorphic Complex in the western part of South Africa forms part of an extensive orogenic belts of mid- to late-Proterozoic age (the Natal-Namaqualand Belt) that is bounded on the northeast by the southern limit of the Archaean Kaapvaal Craton. The study area is located in the southwestern part (the Bushmanland Subprovince) of the Namaqualand Metamorphic Complex (Fig. 1). The area is composed mainly of granitic orthogneiss with amphibolite- to granulite-facies metapelitic gneisses (Waters, 1990). Waters (1989) summarized the progressive

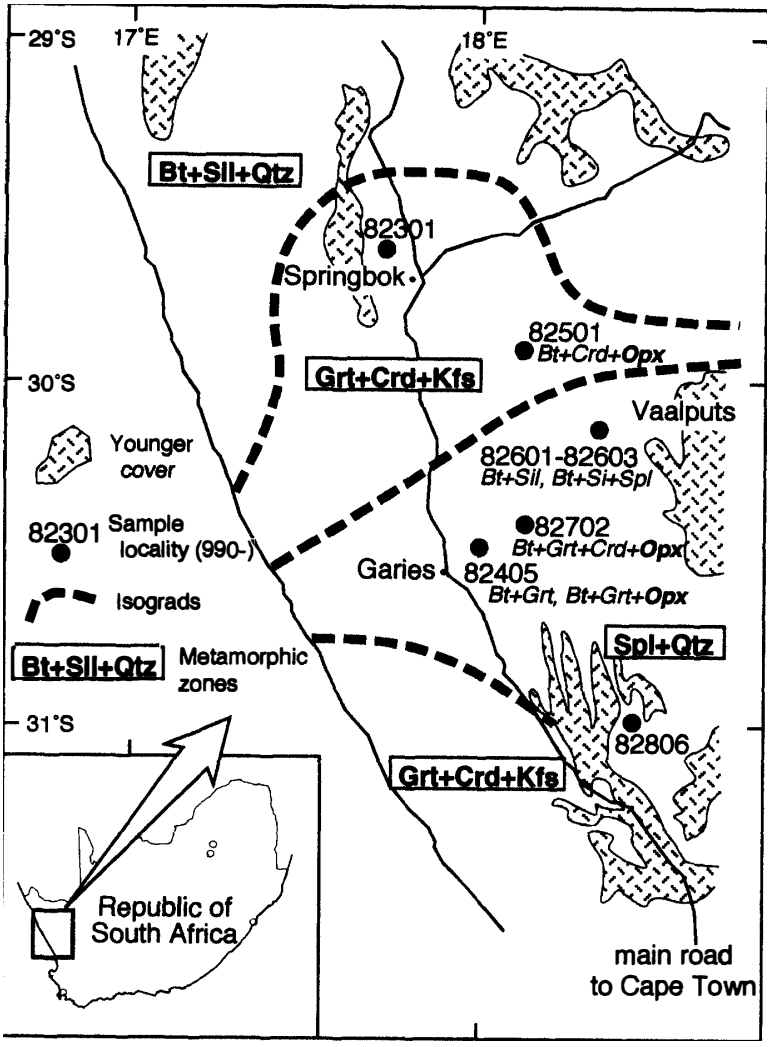

Fig. 1. Geological outline and metamorphic zonation of the study area (after Waters, 1989). Sample localities and mineral parageneses (for ordinary pelitic gneisses) are also shown.

metamorphism of metapelites in the Namaqualand Metamorphic Complex from amphibolite-facies (biotite + sillimanite + quartz) *via.* lower granulite (garnet + cordierite + K-feldspar + quartz) to upper granulite-facies (spinel + quartz). Osumilite has also been reported in magnesian rocks from the highest-grade zone (Nowicki *et al.*, 1995).

Most of the analyzed samples are from the spinel-quartz zone, as the highest-grade zone; the other two (82301 and 82501) are located in the garnet-cordierite-K-feldspar zone in which sapphirine-bearing aluminous gneisses (82301A, 82501C) occur (Fig. 1). Osumilite-bearing gneisses (82806E, G, H) are collected from a small area in the southern part of the spinel-quartz zone, the same locality as reported in Nowicki *et al.* (1995).

3. Petrography

Pelitic gneisses and related rocks analyzed in this study are classified into four types: (1) ordinary pelitic gneiss composed of a combination of biotite, sillimanite, cordierite, garnet, spinel and orthopyroxene in addition to quartz and feldspars but without spinel-quartz or orthopyroxene-sillimanite-quartz coexistences, (2) sapphirine-spinel-corundum-bearing Al and Mg-rich (aluminous) gneiss, (3) osumilite-bearing quartzo-feldspathic Mg-rich (magnesian) gneiss, and (4) magnetite-quartz-bearing Fe-rich (ferruginous) gneiss. Other than these rocks, orthopyroxene-bearing quartzo-feldspathic rock (enderbite), which occurs accompanied by pelitic gneiss, is also described in this paper for comparison to orthopyroxene-bearing metapelitic rocks. Constituent minerals and their chemical features are summarized in Tables 1 and 2.

3.1. Pelitic gneiss

Metamorphic rocks of pelitic origin occur widely in the Namaqualand Metamorphic Complex, though less voluminous than the large amount of granitic rocks. Pelitic gneisses commonly show weak layered structure, which is defined by the alignment of biotite and occasionally by sillimanite (Figs. 2a and 2b). Migmatitic leucocratic veins also develop, and are intercalated with or locally cut the layered structure of pelitic gneisses (Fig. 2c); in some localities, the layered structure is eliminated (Fig. 2d).

Observed mineral assemblages of pelitic gneisses are varied as shown in Table 1. Both orthopyroxene-bearing and orthopyroxene-free assemblages are observed, even in the same locality. Orthopyroxene occurs as granoblastic grains (82501D, 82702C) or idiomorphic porphyroblast (82405B). Orthopyroxene sometimes includes biotite, suggesting that it is formed through the breakdown of biotite. Biotite is the major

Table 1. Constituent minerals of pelitic gneisses and related rocks from the Namaqualand Metamorphic Complex, South Africa.

Sample No.	Rock type	Phase	Qtz	Pl	Kfs	Bt	Crd	Grt	Sil	Opx	Spl	Spr	Crn	Rt	Os	Opaque
990-																
82301A	Aluminous	Spr-Spl-Crn				+	+		(-)	+	+	+	(-)	+		
82405A	Pelitic	Grt	+	+	+	+		+			-					Ilm
82405B	Pelitic	Grt-Opx	+	+	-	+		+		+	+					Mt, Ilm
82501C	Aluminous	Spr-Spl-Crn				+					+	+	(-)			
82501D	Pelitic	Crd-Opx	+	+		+	+			+						
82601B	Pelitic	Sil	+	-		+			+		-					Ht
82602A	Pelitic	Sil	+	+	+	+			+		+					Mt, Ilm
82603A	Ferruginous	Mt-Qtz	+			-			-		+					Mt
82603B	Pelitic	Sil	+			+			+		+					Ht, Mt
82702A	Enderbite	(Opx)	+	+		-				+						Mt, Ilm
82702C	Pelitic	Grt-Crd-Opx	+	+	+	+	+	+		+	+					Ilm
82806E	Magnesian	Os	+	+	-	-	+			-	-				†	Mt, Tl-Ht
82806G	Magnesian	Os	+	+		-	+			-	-				+	Mt, Tl-Ht
82806H	Magnesian	Os	+	+		-	-			-	-				†	Mt, Tl-Ht

+: major, -:minor, (-): inclusion, †: pseudomorph

Mineral abbreviations are as follows. Qtz: quartz, Pl: plagioclase, Kfs: K-feldspar, Bt: biotite, Crd: cordierite, Grt: garnet, Sil: sillimanite, Opx: orthopyroxene, Spl: spinel, Spr: sapphirine, Crn: corundum, Rt: rutile, Os: osumilite.

Table 2. Chemical features of constituent minerals of pelitic gneisses and related rocks from the Namaqualand Metamorphic Complex, South Africa.

Sample No.	Rock	Bt		Crd	Grt	Opx		Spl		Spr	Os
(990-)	type	XMg	*F**	XMg	XMg	XMg	*Al2O3 **	XMg	*ZnO**	XMg	XMg
82301A	A	0.92-0.93	*1.8-2.5*	0.92-0.94		0.81-0.83	*7.6-8.5*	0.65-0.70	*0.1-0.3*	0.84-0.86	
82405A	P	0.58-0.71	*1.1-1.9*		0.33-0.34						
82405B	P	0.54-0.68	*1.3-1.8*		0.22-0.34	0.52-0.53	*6.4-6.6*	0.13-0.15	*5.7-7.4*		
82501C	A	0.78-0.82	*0.0-1.2*					0.58-0.60	*0.3-0.5*	0.78-0.80	
82501D	P	0.72-0.77	*0.6-0.9*			0.65-0.67	*5.7-6.3*				
82601B	P	0.72-0.76	*3.7-3.9*					0.23-0.26	*0.3-1.1*		
82602A	P	0.67-0.71	*3.4-4.2*					0.17-0.20	*2.1-2.7*		
82603A	F	0.77-0.84	*4.5-5.0*					0.27-0.29	*4.9-5.0*		
82603B	P	0.68-0.73	*3.4-5.8*					0.17-0.20	*12.8-13.7*		
82702A	E	0.64-0.67	*0.6-0.8*			0.58-0.63	*1.2-1.9*				
82702C	P	0.63-0.68	*1.4-1.8*	0.78-0.80	0.29-0.39	0.57-0.59	*7.4-8.2*	0.32-0.38	*1.3-1.4*		
82806E	M	0.83-0.89	*0.4-2.7*	0.89-0.90				0.64-0.66	*2.4-3.1*		
82806G	M	0.83-0.91	*1.3-2.0*	0.89-0.90		0.75-0.76	*4.8-6.4*	0.61-0.63	*3.6-3.9*		0.87-0.90
82806H	M	0.82-0.84	*0.7-2.0*	0.90-0.93		0.74-0.78	*5.3-7.0*	0.62-0.63	*2.8-3.0*		

XMg: $Mg/(Mg+Fe^{2+})$, *: wt.%

Abbreviations of rock types are as follows. A: aluminous, P: pelitic, F: ferruginous, E: enderbite, M: magnesian. Mineral abbreviations are the same as in Table 1.

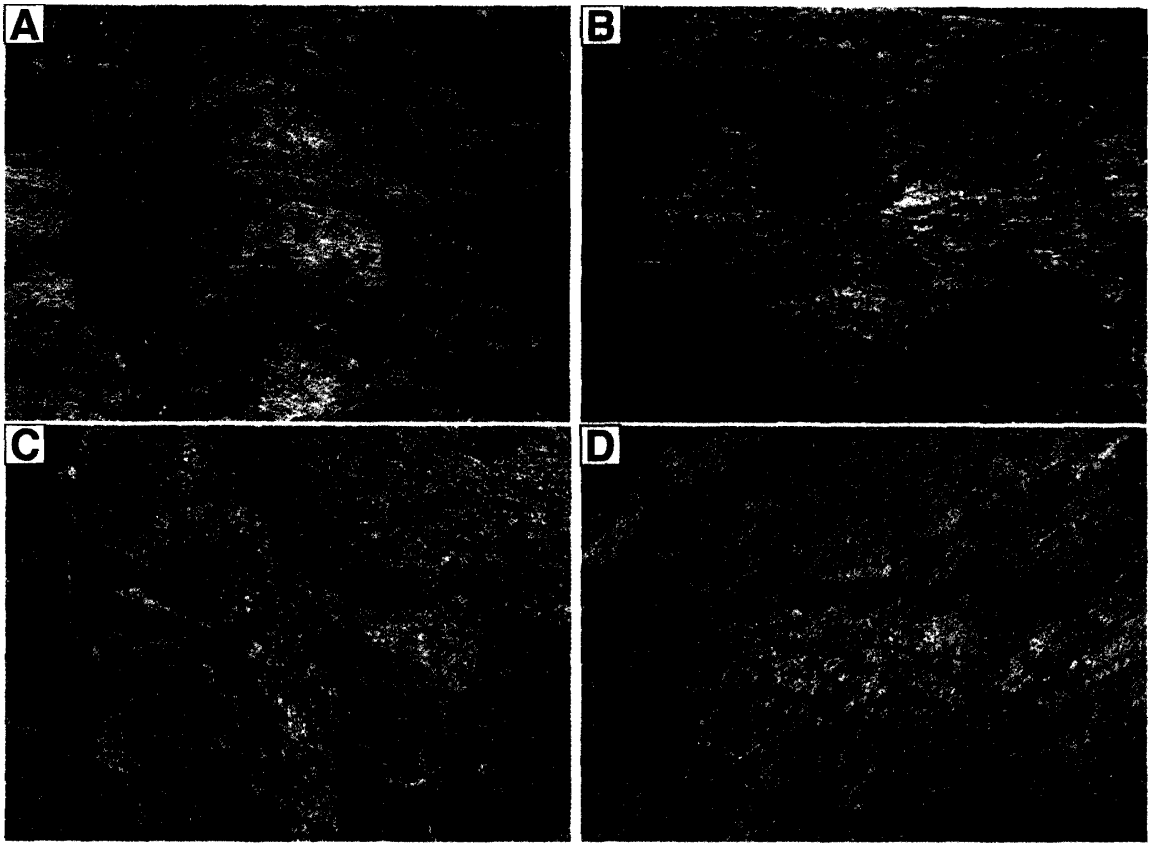

Fig. 2. Pelitic gneisses from the Namaqualand Metamorphic Complex. (a) Typical mode of occurrence of pelitic gneiss. (b) Close up view of (a). Biotite is arranged in parallel to form a layered structure. (c) Migmatitic leucocratic veins occur and locally cut the layered structure of pelitic gneiss. (d) Layered structures of pelitic gneiss are eliminated.

constituent in the pelitic gneisses without exception, even though orthopyroxene is present. Garnet and cordierite are generally granoblastic, and sillimanite is idiomorphic to hypidiomorphic. Spinel is commonly associated with magnetite, ilmenite or rarely hematite; possibly it is an exsolution product from such opaque minerals, whereas it rarely occurs in matrix or as inclusion in garnet or sillimanite. Detailed petrographical features of each sample are described below.

82601B: Biotite-sillimanite gneiss. Relatively fine-grained (<100 μm) spinel-sillimanite-biotite gneiss. Major constituent minerals are quartz, K-feldspar, biotite, sillimanite, spinel and hematite with minor plagioclase (Fig. 3a). Spinel is commonly associated with hematite, and sometimes enclosed within sillimanite.

82602A: Biotite-sillimanite gneiss. Mineral assemblages and mineral textures are similar to 82601B, but opaque minerals are magnetite and ilmenite instead of hematite in 82601B.

82603B: Biotite-sillimanite gneiss. Mineral assemblages and mineral textures are similar to 82601B and 82602A. However, feldspars have not been identified under either optical or electron microscope. Opaque minerals are hematite and magnetite.

82405A: Spinel-garnet-biotite gneiss. Major constituents are quartz, plagioclase, K-feldspar, biotite, garnet and ilmenite. Grain sizes of the constituent minerals are 50–200 μm, except garnet porphyroblast which is up to 5–10 mm in diameter. Garnet includes subhedral biotite and rounded quartz (Fig. 3b). Greenish spinel is commonly associated with ilmenite, or rarely occurs as inclusion in garnet.

82405B: Garnet and orthopyroxene porphyroblast-bearing gneiss. Major constituent minerals are quartz, plagioclase, biotite, garnet, orthopyroxene, magnetite and ilmenite. Orthopyroxene and garnet form porphyroblasts up to 1 cm in diameter, and are of irregular shape or occasionally idiomorphic (Fig. 3c). Green spinel is commonly associated with ilmenite and magnetite.

82501D: Orthopyroxene-cordierite-biotite gneiss. Constituent minerals are quartz, plagioclase, biotite, cordierite and orthopyroxene. Orthopyroxene, 50–100 μm in diameter, occurs as granoblastic grains and is commonly associated with biotite (Fig. 3d). A relatively large amount of cordierite, up to 300 μm in diameter, occurs.

82702C: Garnet-cordierite-orthopyroxene-biotite gneiss. Major constituents are quartz, plagioclase, K-feldspar, garnet, cordierite and orthopyroxene. The opaque mineral is ilmenite, which accompanies spinel. Garnet and orthopyroxene occur in different domains in the gneiss. Garnet is porphyroblastic up to 1 cm, and includes biotite, quartz and ilmenite (Fig. 3e). A thin film of garnet occasionally occurs around ilmenite. Orthopyroxene is granoblastic and is 0.5 to 2 mm in diameter (Fig. 3f).

3.2. Aluminous gneiss

Sapphirine-spinel-corundum-bearing quartz-free aluminous gneiss occurs at two localities in the study area. They occur in several meters to several tens of meters thick layers or blocks, intercalated within quartzite at one locality (82301A, Fig. 4a) and mafic granulite at another (82501C, Fig. 4b). The latter is associated with aluminous gneisses characteristically containing a variety of boronsilicates, such as konerupine, grandidierite and werdingite. It is conspicuous that sapphirine-spinel-corundum aggregate occurs as bluish porphyroblastic clots up to 10 cm in diameter. The detailed petrography of each

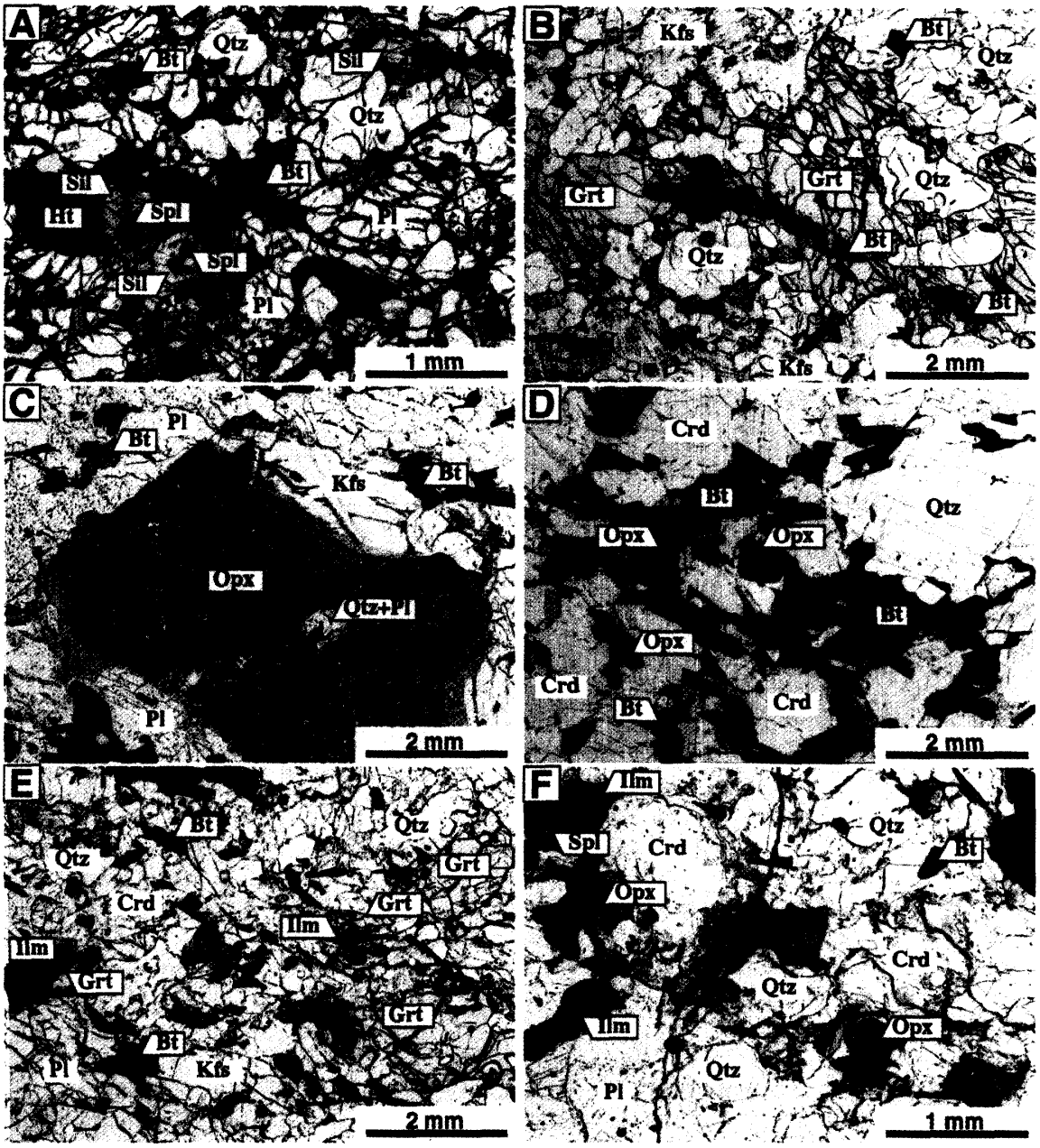

Fig. 3. Photomicrograph of pelitic gneisses. (a) Biotite-sillimanite gneiss (82601B). Spinel is commonly surrounded by sillimanite. (b) Garnet-biotite gneiss (82405A). (c) Garnet-orthopyroxene-porphyroblast-bearing gneiss (82405B). (d) Orthopyroxene-cordierite-biotite gneiss (82501D). (e) Garnet-cordierite-orthopyroxene-biotite gneiss (82702C). Garnet occasionally surrounds ilmenite. (f) The orthopyroxene-rich portion of garnet-cordierite-orthopyroxene-biotite gneiss (82702C). Spinel is commonly associated with ilmenite.

sample is as follows.

82301A: Corundum-spinel-sapphirine-cordierite-orthopyroxene gneiss. Corundum-spinel-sapphirine aggregate of up to 5 cm occurs in orthopyroxene-cordierite matrix (Fig. 4c). Spinel encloses corundum, and both of them are surrounded by sapphirine. Sillimanite occasionally occurs around corundum. Cordierite occurs around the

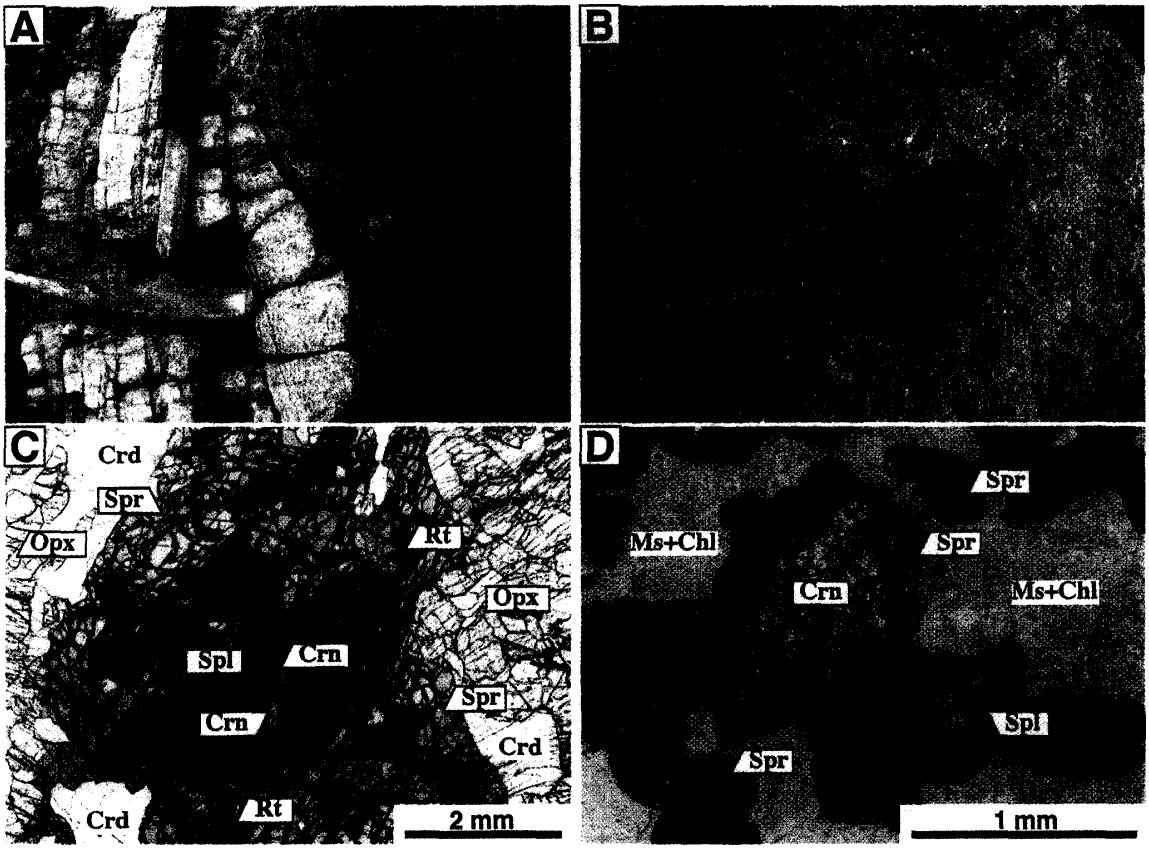

Fig. 4. Sapphirine-bearing aluminous gneisses. (a) Field occurrence of sapphirine-spinel-corundum-orthopyroxene-cordierite gneiss (right-side) interlayered with quartzite (left-side) (82301A). Sapphirine-spinel-corundum aggregate occurs as bluish irregular-shaped clots. (b) Field occurrence of sapphirine-spinel-corundum-biotite gneiss (82501C). (c) Photomicrograph of 82301A. Sapphirine-spinel-corundum aggregate occurs in orthopyroxene-cordierite-bearing matrix. Corundum is enclosed within spinel; both of them are surrounded by sapphirine. (d) Photomicrograph of 82501C. Corundum is commonly surrounded by sapphirine. The matrix is completely altered to a fine-grained aggregate of muscovite and chlorite (labeled 'Ms+Chl').

corundum-spinel-sapphirine aggregate. Biotite (phlogopite) and rutile are minor.

82501C: Corundum-spinel-sapphirine-biotite-gneiss. Corundum-spinel-sapphirine aggregate, up to 5 cm, occurs in the muscovite-chlorite matrix (Fig. 4d). Corundum is surrounded by sapphirine. Spinel is locally present between sapphirine and corundum. Biotite occurs as hypidiomorphic grain or as secondary fine-grained aggregate.

3.3. Osumilite-bearing magnesian gneiss (82608E, G, H)

Osumilite-bearing magnesian gneiss, which has been reported by Nowicki *et al.* (1995), occurs in the southernmost area of the highest-grade (spinel-quartz) zone. It looks bluish green in rock specimens (Fig. 5a). Major constituent minerals are quartz, plagioclase, cordierite, osumilite (pseudomorph) and opaque minerals (magnetite and titano-hematite) with minor biotite, spinel and orthopyroxene. Fine-grained (sub micron-scale) cordierite-K-feldspar-quartz-orthopyroxene symplectite (labeled 'Symp' in Figs. 5c and 5d), which is probably pseudomorph after osumilite, occurs in a large proportion of

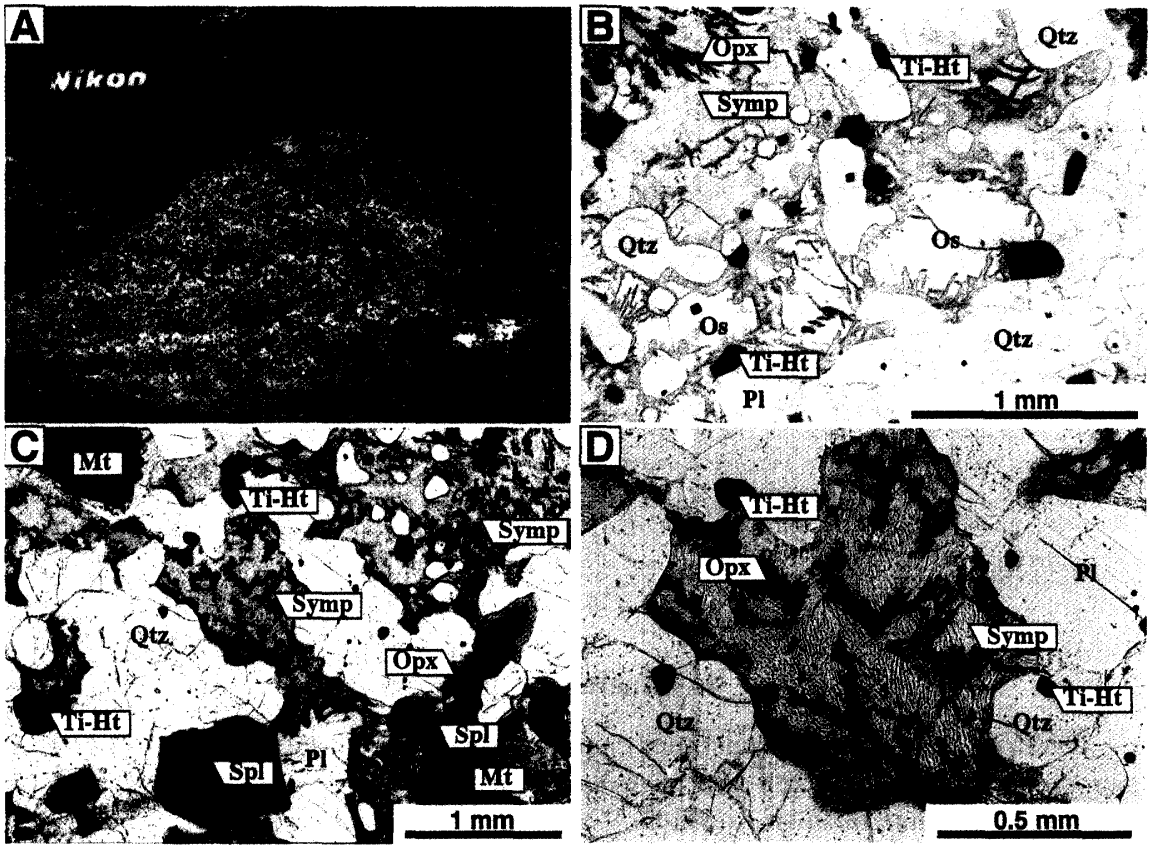

Fig. 5. (a) Field occurrence of osumilite-bearing magnesian gneiss. Dark-colored clots are magnetite porphyroblasts. (b) Photomicrograph of osumilite-bearing gneiss (82806G). (c) Photomicrograph of osumilite-bearing gneiss (82806H). Osumilite (pseudomorph) is replaced by a fine-scale symplectite (labeled 'Symp') of cordierite-K-feldspar-quartz-orthopyroxene. Magnetite is occasionally surrounded by a thin film of orthopyroxene. (d) Close up view of the osumilite-pseudomorph as in (c).

the gneiss. Only a trace of osumilite survives in the sample 82806G (Fig. 5b). Osumilite is rounded, and surrounded (possibly replaced) by fine-grained symplectite. Spinel is commonly associated with magnetite, and spinel-magnetite aggregate is sometimes surrounded by fine-grained orthopyroxene film (Fig. 5c).

3.4. Ferruginous (magnetite-quartz) gneiss (82603A)

Magnetite-quartz gneiss, possibly a meta-iron stone, occurs intercalated with pelitic gneiss. It is composed of quartz, magnetite, spinel and sillimanite with minor biotite (Fig. 6a). Magnetite, up to 5 mm in diameter, is xenomorphic, and commonly accompanies dark green spinel. Sillimanite also occurs as hypidiomorphic grain and includes spinel.

3.5. Enderbite (82702A)

Enderbite, interlayered with pelitic gneiss, is composed of quartz, plagioclase and orthopyroxene. It shows granoblastic texture (Fig. 6b). A trace amount of biotite is present locally in matrix or as inclusion in orthopyroxene. The opaque mineral is magnetite.

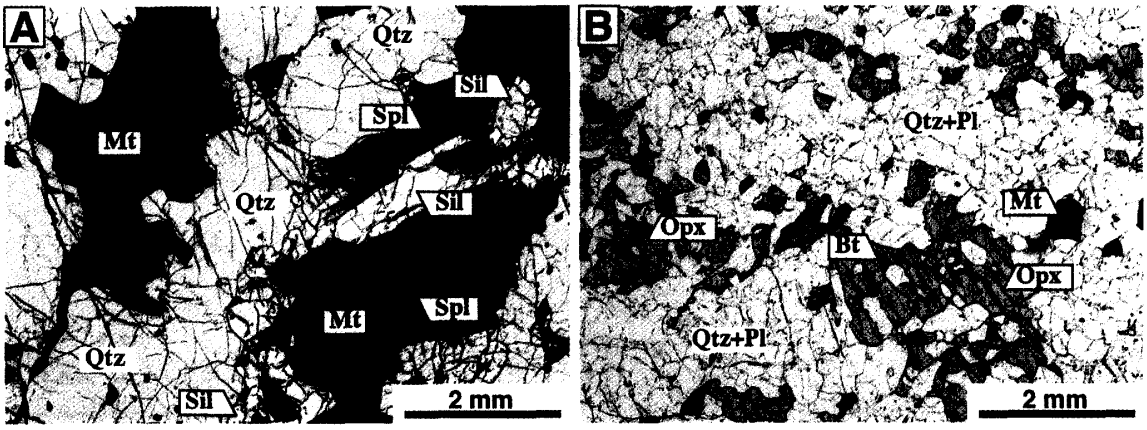

Fig. 6. (a) Photomicrograph of magnetite-quartz-rich ferruginous gneiss (82603A). Spinel is commonly associated with magnetite. Magnetite is occasionally surrounded by sillimanite. (b) Photomicrograph of enderbite (82702A). Fine-grained biotite is present as inclusion in orthopyroxene.

4. Mineral chemistry

Chemical analyses of constituent minerals were performed using an electron microprobe with a wavelength-dispersive X-ray analytical system (JEOL JXA-8800M) at the National Institute of Polar Research. Oxide ZAF correction was applied to analyses. Probe current was kept at about 8–12 nA with accelerating voltage at 15 kV. Synthesized pure oxides and natural minerals were used for standards. Chemical features and representative analyses of constituent minerals are summarized in Tables 2 and 3.

4.1. Biotite

Mg/(Mg+Fe) ratios of biotite in ordinary pelitic gneisses range from 0.54 to 0.77, while those in aluminous, ferruginous and magnesian gneisses range from 0.77 to 0.93. Fluorine contents in biotite change with sample localities, and are not correlated with coexisting minerals (Fig. 7), 1.8–2.5 wt% (82301), 1.1–1.9 wt% (82405), 0.0–1.2 wt% (82501), 3.4–5.8 wt% (82601–82603), 0.6–1.8 wt% (82702), and 0.4–2.7 wt% (82806).

4.2. Orthopyroxene

Mg/(Mg+Fe) ratios of orthopyroxene from ordinary pelitic gneisses range from 0.52 to 0.67, but those from sapphirine-bearing and osumilite-bearing aluminous and magnesian gneisses range from 0.74 to 0.85. Al_2O_3 contents of orthopyroxene from pelitic, aluminous and magnesian gneiss range from 4.8 to 8.2 wt%, which is markedly higher than that from enderbite showing 1.2–1.9 wt% (Fig. 8a). Orthopyroxene in pelitic gneisses show weak compositional zoning, and the highest Al_2O_3 content up to 8.5 wt% is recorded in the core.

4.3. Spinel

Spinel from sapphirine-bearing and osumilite-bearing aluminous and magnesian gneisses shows $Mg/(Mg+Fe^{2+})$ ratios from 0.58 to 0.70 with ZnO content less than 0.5 wt%

Table 3. Representative elctron microprobe analyses of constituent minerals. Abbreviations of rock types are the same as in Table 2.

Mineral	Orthopyroxene							Sapphirine			
Sample	82301A	82405B	82501D	82702A	82702C	82806G	82806H	82301A	82301A	82501C	82501C
Rock type	A	P	P	E	P	M	M	A	A	A	A
SiO_2	32.37	47.34	50.03	51.85	46.81	51.27	50.83	14.12	14.52	11.27	12.45
TiO_2	0.24	0.15	0.02	0.10	0.07	0.13	0.10	0.09	0.14	0.04	0.06
Al_2O_3	8.50	6.64	6.27	1.92	8.21	6.43	7.61	61.89	61.44	64.41	63.17
Cr_2O_3	0.00	0.00	0.00	0.02	0.01	0.00	0.00	0.06	0.06	0.00	0.03
FeO*	11.01	27.18	19.69	24.45	25.01	15.13	14.99	6.03	5.17	8.19	7.83
MnO	0.09	0.33	0.85	0.62	0.23	1.42	1.17	0.02	0.00	0.12	0.17
ZnO	0.00	0.00	0.06	0.18	0.02	0.09	0.05	0.00	0.15	0.00	0.00
MgO	29.51	17.40	22.67	21.42	18.93	25.59	26.08	18.64	18.48	16.40	16.83
CaO	0.07	0.09	0.11	0.39	0.06	0.10	0.04	0.01	0.02	0.01	0.00
Na_2O	0.00	0.01	0.04	0.02	0.00	0.00	0.01	0.04	0.01	0.01	0.02
K_2O	0.00	0.00	0.00	0.00	0.00	0.00	0.00	0.00	0.00	0.00	0.00
Total	101.79	99.14	99.73	100.97	99.35	100.16	100.87	100.90	99.98	100.45	100.55
Cations	(O=6)							(O=20)			
Si	1.811	1.824	1.848	1.935	1.782	1.850	1.818	1.654	1.709	1.343	1.478
Ti	0.006	0.004	0.001	0.003	0.002	0.004	0.003	0.008	0.012	0.004	0.005
Al	0.346	0.301	0.273	0.084	0.368	0.273	0.321	8.543	8.522	9.043	8.837
Cr	0.000	0.000	0.000	0.000	0.000	0.000	0.000	0.006	0.006	0.000	0.003
Fe	0.318	0.876	0.608	0.763	0.796	0.457	0.448	0.590	0.509	0.816	0.777
Mn	0.003	0.011	0.027	0.020	0.007	0.043	0.035	0.002	0.000	0.012	0.017
Zn	0.000	0.000	0.002	0.005	0.001	0.002	0.001	0.000	0.013	0.000	0.000
Mg	1.522	0.999	1.249	1.192	1.074	1.377	1.390	3.255	3.242	2.913	2.978
Ca	0.003	0.004	0.004	0.016	0.002	0.004	0.002	0.001	0.003	0.001	0.000
Na	0.000	0.001	0.003	0.001	0.000	0.000	0.001	0.009	0.002	0.002	0.005
K	0.000	0.000	0.000	0.000	0.000	0.000	0.000	0.000	0.000	0.000	0.000
Total	4.009	4.020	4.015	4.019	4.032	4.010	4.019	14.068	14.018	14.134	14.100
Mg/(Mg+Fe)	0.827	0.533	0.673	0.610	0.574	0.751	0.756	0.847	0.864	0.781	0.793
Fe^{3+} **	0.032	0.051	0.031	0.046	0.068	0.027	0.043	0.149	0.060	0.271	0.207
Fe^{2+} **	0.286	0.825	0.577	0.717	0.728	0.430	0.405	0.441	0.449	0.545	0.570
$Mg/(Mg+Fe^{2+})$	0.842	0.548	0.684	0.624	0.596	0.762	0.774	0.881	0.878	0.842	0.839
Fe^{3+}/Total Fe	0.101	0.058	0.051	0.060	0.085	0.059	0.096	0.253	0.118	0.332	0.266

* Total Fe as FeO, ** Calculated from stoichiometry

Mineral	Spinel										
Sample	82301A	82405B	82501C	82601B	82602A	82603A	82603B	82702C	82806E	82806G	82806H
Rock type	A	P	A	P	P	F	P	P	M	M	M
SiO_2	0.01	0.00	0.00	0.02	0.05	0.00	0.04	0.00	0.03	0.00	0.05
TiO_2	0.05	0.20	0.00	0.01	0.00	0.00	0.15	0.06	0.02	0.03	0.02
Al_2O_3	66.00	57.23	63.77	58.37	59.17	59.17	59.63	60.10	65.35	63.63	65.10
Cr_2O_3	0.09	1.21	0.00	0.09	0.00	0.00	0.00	0.58	0.43	0.36	0.43
FeO*	15.70	31.14	19.48	35.55	33.84	27.81	23.18	31.13	14.64	16.56	15.73
MnO	0.16	0.12	0.31	0.51	1.40	1.19	1.15	0.03	0.92	0.73	0.96
ZnO	0.09	7.43	0.35	0.33	2.29	4.98	12.78	1.35	3.13	3.85	2.97
MgO	18.48	2.63	15.98	6.16	4.03	6.42	3.31	8.07	15.84	14.40	14.76
CaO	0.00	0.02	0.00	0.00	0.00	0.01	0.01	0.01	0.02	0.00	0.00
Na_2O	0.02	0.24	0.01	0.03	0.06	0.20	0.35	0.05	0.09	0.10	0.06
K_2O	0.00	0.00	0.00	0.00	0.00	0.00	0.00	0.00	0.00	0.00	0.00
Total	100.60	100.22	99.90	101.07	100.84	99.78	100.60	101.37	100.47	99.66	100.08
Cations	(O=4)										
Si	0.000	0.000	0.000	0.001	0.001	0.000	0.001	0.000	0.001	0.000	0.001
Ti	0.001	0.004	0.000	0.000	0.000	0.000	0.003	0.001	0.000	0.001	0.000
Al	1.972	1.945	1.960	1.925	1.965	1.960	1.995	1.938	1.985	1.976	1.993
Cr	0.002	0.028	0.000	0.002	0.000	0.000	0.000	0.013	0.009	0.007	0.009
Fe	0.333	0.751	0.425	0.832	0.797	0.654	0.550	0.712	0.316	0.365	0.342
Mn	0.003	0.003	0.007	0.012	0.033	0.028	0.028	0.001	0.020	0.016	0.021
Zn	0.002	0.158	0.007	0.007	0.048	0.103	0.268	0.027	0.060	0.075	0.057
Mg	0.699	0.113	0.621	0.257	0.169	0.269	0.140	0.329	0.609	0.566	0.572
Ca	0.000	0.001	0.000	0.000	0.000	0.000	0.000	0.000	0.001	0.000	0.000
Na	0.001	0.013	0.001	0.002	0.003	0.011	0.019	0.003	0.004	0.005	0.003
K	0.000	0.000	0.000	0.000	0.000	0.000	0.000	0.000	0.000	0.000	0.000
Total	3.013	3.016	3.021	3.038	3.017	3.025	3.004	3.024	3.005	3.011	2.998
Mg/(Mg+Fe)	0.677	0.131	0.594	0.236	0.175	0.291	0.203	0.316	0.658	0.608	0.626
Fe^{3+} **	0.028	0.055	0.040	0.075	0.035	0.040	0.005	0.062	0.015	0.024	0.007
Fe^{2+} **	0.305	0.696	0.385	0.757	0.762	0.614	0.545	0.650	0.301	0.341	0.335
$Mg/(Mg+Fe^{2+})$	0.696	0.140	0.617	0.253	0.182	0.305	0.204	0.336	0.669	0.624	0.631
Fe^{3+}/Total Fe	0.084	0.073	0.094	0.090	0.044	0.061	0.009	0.087	0.047	0.066	0.020

* Total Fe as FeO, ** Calculated from stoichiometry

Table 3 (continued).

Mineral	Osumilite	Cordierite					Biotite				
Sample	82806G	82806G	82806G	82301A	82702C	82806E	82806G	82806H	82301A	82405A	82405B
Rock type	M	M	M	A	P	M	M	M	A	P	P
SiO_2	62.58	63.03	62.55	51.31	49.39	50.01	50.27	50.96	41.20	37.93	36.52
TiO_2	0.13	0.07	0.08	0.00	0.05	0.06	0.00	0.00	2.11	3.37	4.40
Al_2O_3	22.04	22.35	22.48	34.46	33.50	34.14	34.06	33.98	14.92	15.36	14.82
Cr_2O_3	0.01	0.01	0.06	0.03	0.00	0.04	0.00	0.00	0.03	0.16	0.08
FeO*	1.71	1.79	2.01	1.66	4.61	2.56	2.49	2.39	3.72	11.86	15.58
MnO	0.15	0.10	0.20	0.00	0.09	0.18	0.23	0.18	0.02	0.02	0.06
ZnO	0.00	0.00	0.04	0.00	0.07	0.06	0.00	0.02	0.03	0.03	0.01
MgO	8.50	7.83	8.26	12.71	10.49	12.07	11.98	12.44	23.67	16.29	13.95
CaO	0.01	0.01	0.00	0.05	0.00	0.00	0.02	0.00	0.00	0.04	0.00
Na_2O	0.38	0.29	0.37	0.06	0.22	0.11	0.10	0.11	0.60	0.18	0.07
K_2O	4.51	4.35	4.40	0.00	0.00	0.00	0.00	0.00	9.24	9.94	9.71
F									2.50	1.85	1.77
-O									-1.05	-0.78	-0.75
Total	100.02	99.83	100.45	100.28	98.41	99.23	99.15	100.08	96.98	96.25	96.22
Cations	(O=30)			(O=18)					(O=22)		
Si	10.322	10.383	10.285	5.019	4.997	4.974	4.999	5.018	5.778	5.596	5.496
Ti	0.016	0.009	0.010	0.000	0.004	0.004	0.000	0.000	0.222	0.374	0.498
Al	4.284	4.339	4.356	3.973	3.994	4.001	3.992	3.943	2.466	2.671	2.629
Cr	0.001	0.001	0.008	0.002	0.000	0.003	0.000	0.000	0.003	0.019	0.010
Fe	0.236	0.247	0.276	0.136	0.390	0.213	0.207	0.196	0.436	1.463	1.961
Mn	0.021	0.014	0.028	0.000	0.008	0.015	0.019	0.015	0.002	0.002	0.008
Zn	0.000	0.000	0.005	0.000	0.005	0.004	0.000	0.001	0.003	0.003	0.001
Mg	2.090	1.923	2.024	1.853	1.582	1.790	1.776	1.826	4.948	3.583	3.130
Ca	0.002	0.002	0.000	0.005	0.000	0.000	0.002	0.000	0.000	0.006	0.000
Na	0.122	0.091	0.118	0.011	0.043	0.021	0.019	0.021	0.163	0.051	0.020
K	0.949	0.914	0.923	0.000	0.000	0.000	0.000	0.000	1.653	1.871	1.864
Total	18.043	17.923	18.033	10.999	11.024	11.026	11.014	11.021	15.674	15.640	15.617
F									1.109	0.863	0.842
Mg/(Mg+Fe)	0.899	0.886	0.880	0.932	0.802	0.894	0.896	0.903	0.919	0.710	0.615
F/(F+OH)									0.277	0.216	0.211

* Total Fe as FeO

Mineral	Biotite										
Sample	82501C	82501D	82601B	82602A	82603A	82603B	82702A	82702C	82806E	82806G	82806H
Rock type	A	P	P	P	F	P	E	P	M	M	M
SiO_2	37.84	37.31	38.19	37.89	40.00	38.21	36.47	36.56	39.27	39.31	39.68
TiO_2	2.77	2.33	4.89	4.00	2.31	2.35	5.50	6.06	3.02	3.92	4.51
Al_2O_3	17.85	17.08	14.41	14.93	14.37	14.40	13.41	14.54	14.79	14.92	14.16
Cr_2O_3	0.00	0.08	0.02	0.00	0.00	0.00	0.04	0.01	0.00	0.00	0.10
FeO*	7.20	11.63	10.72	11.97	7.45	11.99	13.23	14.64	5.29	7.07	6.70
MnO	0.04	0.09	0.05	0.29	0.11	0.39	0.06	0.01	0.12	0.11	0.14
ZnO	0.00	0.00	0.13	0.00	0.20	0.15	0.02	0.07	0.00	0.01	0.05
MgO	18.26	16.42	17.40	16.66	21.18	17.62	15.08	13.96	22.01	19.31	20.00
CaO	0.00	0.04	0.00	0.00	0.00	0.00	0.06	0.00	0.00	0.00	0.02
Na_2O	0.42	0.27	0.14	0.13	0.20	0.19	0.04	0.17	0.09	0.13	0.10
K_2O	9.30	9.29	9.87	9.62	9.97	9.96	9.05	9.64	10.11	10.29	10.31
F	1.16	0.86	3.94	4.15	4.92	5.77	0.82	1.81	2.65	1.95	1.53
-O	-0.49	-0.36	-1.66	-1.75	-2.07	-2.43	-0.35	-0.76	-1.12	-0.84	-0.64
Total	94.35	95.03	98.08	97.89	98.63	98.59	93.43	96.69	96.23	96.18	96.65
Cations	(O=22)										
Si	5.513	5.508	5.576	5.574	5.734	5.652	5.554	5.458	5.642	5.675	5.685
Ti	0.304	0.259	0.537	0.443	0.249	0.261	0.630	0.680	0.326	0.426	0.486
Al	3.065	2.972	2.479	2.588	2.428	2.510	2.407	2.557	2.503	2.539	2.391
Cr	0.000	0.009	0.002	0.000	0.000	0.000	0.005	0.001	0.000	0.000	0.011
Fe	0.877	1.436	1.308	1.472	0.893	1.482	1.685	1.828	0.635	0.854	0.803
Mn	0.005	0.011	0.006	0.036	0.013	0.048	0.008	0.001	0.015	0.013	0.016
Zn	0.000	0.000	0.014	0.000	0.021	0.016	0.002	0.008	0.000	0.001	0.005
Mg	3.966	3.614	3.786	3.653	4.525	3.885	3.424	3.107	4.714	4.156	4.272
Ca	0.000	0.006	0.000	0.000	0.000	0.000	0.010	0.000	0.000	0.000	0.003
Na	0.119	0.077	0.038	0.037	0.056	0.054	0.012	0.049	0.025	0.036	0.028
K	1.728	1.750	1.837	1.805	1.823	1.879	1.758	1.836	1.853	1.895	1.884
Total	15.575	15.642	15.584	15.609	15.742	15.789	15.495	15.525	15.713	15.595	15.584
F	0.534	0.401	1.819	1.931	2.230	2.696	0.395	0.855	1.204	0.890	0.693
Mg/(Mg+Fe)	0.819	0.716	0.743	0.713	0.835	0.724	0.670	0.630	0.881	0.830	0.842
F/(F+OH)	0.134	0.100	0.455	0.483	0.558	0.674	0.099	0.214	0.301	0.223	0.173

* Total Fe as FeO

Table 3 (continued).

Mineral	Garnet							Mineral	Plagioclase		
Sample	82405A	82405B	82405B	82405B	82702C	82702C	82702C	Sample	82405A	82405B	82501D
Rock type	P	P	P	P	P	P	P	Rock type	P	P	P
		core	rim	film	core	rim	film				
SiO_2	39.25	38.03	37.94	37.16	38.94	39.28	38.28	SiO_2	61.28	59.12	59.15
TiO_2	0.00	0.04	0.02	0.00	0.03	0.01	0.06	TiO_2	0.00	0.01	0.00
Al_2O_3	22.23	21.78	22.11	21.37	22.39	22.39	21.88	Al_2O_3	24.55	25.48	25.73
Cr_2O_3	0.07	0.05	0.02	0.04	0.00	0.00	0.00	Cr_2O_3	0.01	0.01	0.06
FeO*	29.82	30.05	30.66	31.11	27.60	27.36	31.65	FeO*	0.01	0.19	0.18
MnO	0.72	1.50	1.63	3.58	0.62	0.69	0.76	MnO	0.00	0.00	0.00
ZnO	0.00	0.03	0.00	0.00	0.08	0.04	0.00	ZnO	0.00	0.00	0.00
MgO	8.29	8.20	7.40	4.78	9.76	9.63	7.36	MgO	0.01	0.00	0.00
CaO	1.10	0.85	0.99	2.13	0.97	1.06	0.93	CaO	5.65	6.74	6.87
Na_2O	0.01	0.00	0.01	0.00	0.00	0.01	0.00	Na_2O	8.64	8.24	7.96
K_2O	0.00	0.00	0.00	0.00	0.00	0.00	0.00	K_2O	0.15	0.11	0.13
Total	101.49	100.53	100.78	100.16	100.39	100.47	100.92	P_2O_5	0.08	0.14	0.04
Cations	(O=12)							Total	100.38	100.04	100.12
Si	2.999	2.955	2.950	2.959	2.978	2.999	2.975	Cations	(O=8)		
Ti	0.000	0.002	0.001	0.000	0.002	0.001	0.004	Si	2.713	2.642	2.640
Al	2.002	1.995	2.026	2.005	2.018	2.015	2.004	Ti	0.000	0.000	0.000
Cr	0.004	0.003	0.001	0.002	0.000	0.000	0.000	Al	1.281	1.342	1.353
Fe	1.905	1.953	1.994	2.071	1.765	1.747	2.057	Cr	0.000	0.000	0.002
Mn	0.047	0.099	0.107	0.241	0.040	0.045	0.050	Fe	0.000	0.007	0.007
Zn	0.000	0.002	0.000	0.000	0.005	0.002	0.000	Mn	0.000	0.000	0.000
Mg	0.944	0.950	0.858	0.568	1.113	1.096	0.853	Zn	0.000	0.000	0.000
Ca	0.090	0.071	0.082	0.182	0.079	0.087	0.077	Mg	0.001	0.000	0.000
Na	0.001	0.000	0.002	0.000	0.000	0.001	0.000	Ca	0.268	0.323	0.328
K	0.000	0.000	0.000	0.000	0.000	0.000	0.000	Na	0.742	0.714	0.689
Total	7.991	8.029	8.022	8.029	7.999	7.993	8.019	K	0.008	0.006	0.007
Mg/(Mg+Fe)	0.331	0.327	0.301	0.215	0.387	0.386	0.293	P	0.003	0.005	0.002
alm	0.638	0.636	0.656	0.676	0.589	0.587	0.677	Total	5.017	5.039	5.028
prp	0.316	0.309	0.282	0.185	0.371	0.369	0.281	an	0.263	0.309	0.321
grs	0.030	0.023	0.027	0.059	0.027	0.029	0.025	ab	0.728	0.685	0.672
sps	0.016	0.032	0.035	0.079	0.013	0.015	0.016	or	0.008	0.006	0.007

* Total Fe as FeO

* Total Fe as FeO n.a.: not analyzed

Mineral	Plagioclase						K-feldspar				
Sample	82602A	82702A	82702C	82806E	82806G	82806H	82602A	82702C	82806E	82806G	82806H
Rock type	P	E	P	M	M	M	P	P	M	M	M
SiO_2	62.24	45.75	59.53	58.23	58.86	58.89	64.54	64.14	63.68	64.12	65.44
TiO_2	0.04	0.03	0.02	0.04	0.00	0.00	0.03	0.06	0.03	0.07	0.03
Al_2O_3	23.70	33.97	25.29	26.37	26.32	26.38	18.73	18.90	18.96	18.60	18.51
Cr_2O_3	0.00	0.01	0.00	0.01	0.03	0.03	0.00	0.06	0.01	0.06	0.04
FeO*	0.21	0.33	0.04	0.08	0.17	0.00	0.01	0.01	0.07	0.03	0.09
MnO	0.08	0.00	0.06	0.00	0.00	0.00	0.03	0.03	0.00	0.00	0.05
ZnO	0.15	0.08	0.00	0.12	0.08	0.00	0.05	0.01	0.07	0.04	0.03
MgO	0.01	0.05	0.00	0.00	0.00	0.02	0.00	0.01	0.00	0.00	0.01
CaO	4.54	17.45	6.47	7.86	7.98	7.55	0.12	0.15	0.34	0.01	0.00
Na_2O	8.73	1.61	7.92	7.09	7.20	7.16	1.57	1.95	1.87	1.03	1.46
K_2O	0.32	0.07	0.22	0.22	0.22	0.24	14.29	13.73	13.91	15.27	14.35
P_2O_5	0.00	0.01	0.03	0.19	0.10	n.a.	0.04	0.07	0.20	0.06	n.a.
Total	100.02	99.34	99.58	100.21	100.95	100.27	99.41	99.12	99.13	99.29	100.01
Cations	(O=8)						(O=8)				
Si	2.761	2.124	2.665	2.600	2.611	2.622	2.982	2.968	2.953	2.979	3.002
Ti	0.001	0.001	0.001	0.001	0.000	0.000	0.001	0.002	0.001	0.002	0.001
Al	1.239	1.859	1.334	1.388	1.376	1.384	1.020	1.031	1.036	1.018	1.001
Cr	0.000	0.000	0.000	0.000	0.001	0.001	0.000	0.002	0.000	0.002	0.001
Fe	0.008	0.013	0.001	0.003	0.006	0.000	0.000	0.000	0.003	0.001	0.003
Mn	0.003	0.000	0.002	0.000	0.000	0.000	0.001	0.001	0.000	0.000	0.002
Zn	0.005	0.003	0.000	0.004	0.002	0.000	0.002	0.000	0.002	0.001	0.001
Mg	0.001	0.003	0.000	0.000	0.000	0.001	0.000	0.001	0.000	0.000	0.001
Ca	0.216	0.868	0.310	0.376	0.379	0.360	0.006	0.007	0.017	0.000	0.000
Na	0.751	0.144	0.687	0.614	0.619	0.618	0.141	0.175	0.168	0.093	0.130
K	0.018	0.004	0.013	0.013	0.012	0.014	0.842	0.811	0.823	0.905	0.839
P	0.000	0.000	0.001	0.007	0.004	-	0.002	0.003	0.008	0.002	-
Total	5.002	5.019	5.015	5.007	5.010	5.001	4.996	5.002	5.011	5.003	4.981
an	0.219	0.854	0.307	0.375	0.375	0.363	0.006	0.007	0.017	0.000	0.000
ab	0.762	0.142	0.680	0.612	0.613	0.623	0.142	0.176	0.167	0.093	0.134
or	0.018	0.004	0.012	0.013	0.012	0.014	0.852	0.816	0.816	0.907	0.866

Table 3 (continued).

Mineral	Ilmenite					Magnetite				
Sample	82405A	82405B	82602A	82702A	82702C	82405B	82602A	82603A	82603B	82702A
Rock type	P	P	P	E	P	P	P	F	P	E
SiO_2	0.00	0.04	0.01	0.02	0.00	0.01	0.02	0.03	0.09	0.05
TiO_2	49.68	50.78	53.26	52.30	50.14	0.08	3.95	0.17	0.65	0.09
Al_2O_3	0.00	0.00	0.05	0.01	0.00	0.10	0.77	0.28	0.63	0.09
Cr_2O_3	0.18	0.04	0.00	0.02	0.07	0.43	0.00	0.01	0.03	0.30
Fe_2O_3	0.00	0.00	0.00	0.00	0.00	68.22	65.07	68.48	67.39	67.93
FeO	48.86	45.83	36.48	47.03	48.11	30.69	29.27	30.81	30.32	30.56
MnO	0.23	3.17	8.68	1.24	0.54	0.11	0.63	0.10	0.10	0.05
ZnO	0.00	0.04	0.03	0.02	0.05	0.00	0.00	0.16	0.00	0.00
MgO	0.15	0.14	0.03	0.25	0.19	0.00	0.00	0.03	0.02	0.02
CaO	0.00	0.00	0.00	0.00	0.00	0.03	0.00	0.01	0.01	0.01
Na_2O	0.00	0.02	0.01	0.01	0.02	0.00	0.01	0.05	0.01	0.00
K_2O	0.00	0.00	0.00	0.00	0.00	0.00	0.00	0.00	0.00	0.00
Total	99.10	100.05	98.55	100.90	99.12	99.67	99.72	100.13	99.25	99.09
Cations	(O=3)					(O=4)				
Si	0.000	0.001	0.000	0.001	0.000	0.000	0.001	0.001	0.003	0.002
Ti	0.964	0.973	1.017	0.987	0.971	0.002	0.112	0.005	0.019	0.003
Al	0.000	0.000	0.001	0.000	0.000	0.005	0.034	0.013	0.029	0.004
Cr	0.004	0.001	0.000	0.000	0.001	0.013	0.000	0.000	0.001	0.009
Fe^{3+}	0.000	0.000	0.000	0.000	0.000	1.980	1.851	1.978	1.953	1.982
Fe^{2+}	1.054	0.976	0.774	0.987	1.036	0.990	0.925	0.989	0.976	0.991
Mn	0.005	0.068	0.187	0.026	0.012	0.004	0.020	0.003	0.003	0.002
Zn	0.000	0.001	0.001	0.000	0.001	0.000	0.000	0.005	0.000	0.000
Mg	0.006	0.005	0.001	0.009	0.007	0.000	0.000	0.002	0.001	0.001
Ca	0.000	0.000	0.000	0.000	0.000	0.001	0.000	0.000	0.000	0.000
Na	0.000	0.001	0.000	0.000	0.001	0.000	0.001	0.004	0.001	0.000
K	0.000	0.000	0.000	0.000	0.000	0.000	0.000	0.000	0.000	0.000
Total	2.033	2.026	1.982	2.012	2.029	2.995	2.944	3.000	2.987	2.994
XFe^{3+}/Total Fe	0.000	0.000	0.000	0.000	0.000	0.667	0.667	0.667	0.667	0.667

Mineral	Magnetite			Hematite		Titano-hematite		
Sample	82806E	82806G	82806H	82601B	82603B	82806E	82806G	82806H
Rock type	M	M	M	P	P	M	M	M
SiO_2	0.04	0.06	0.00	0.24	0.27	0.01	0.02	0.02
TiO_2	0.00	0.06	0.00	0.06	0.29	13.40	19.04	16.77
Al_2O_3	0.09	0.12	0.13	0.46	0.17	0.10	0.04	0.26
Cr_2O_3	0.28	0.40	0.30	0.12	0.00	0.11	0.16	0.10
Fe_2O_3	68.70	67.12	68.74	97.53	98.98	86.62	78.95	81.91
FeO	30.91	30.19	30.93	0.00	0.00	0.00	0.00	0.00
MnO	0.00	0.09	0.00	0.06	0.03	0.74	0.87	1.58
ZnO	0.01	0.00	0.01	0.14	0.00	0.00	0.02	0.02
MgO	0.00	0.00	0.01	0.02	0.00	0.05	0.07	0.33
CaO	0.01	0.00	0.00	0.00	0.01	0.00	0.00	0.02
Na_2O	0.02	0.00	0.00	0.00	0.00	0.00	0.06	0.00
K_2O	0.00	0.00	0.00	0.00	0.00	0.00	0.00	0.00
Total	100.06	98.03	100.12	98.63	99.74	101.03	99.23	101.00
Cations	(O=4)			(O=3)		(O=3)		
Si	0.002	0.002	0.000	0.006	0.007	0.000	0.000	0.000
Ti	0.000	0.002	0.000	0.001	0.006	0.254	0.361	0.315
Al	0.004	0.005	0.006	0.014	0.005	0.003	0.001	0.008
Cr	0.009	0.012	0.009	0.003	0.000	0.002	0.003	0.002
Fe^{3+}	1.988	1.981	1.988	1.962	1.975	1.644	1.498	1.539
Fe^{2+}	0.994	0.990	0.994	0.000	0.000	0.000	0.000	0.000
Mn	0.000	0.003	0.000	0.001	0.001	0.016	0.019	0.033
Zn	0.000	0.000	0.000	0.003	0.000	0.000	0.000	0.000
Mg	0.000	0.000	0.001	0.001	0.000	0.002	0.003	0.012
Ca	0.000	0.000	0.000	0.000	0.000	0.000	0.000	0.001
Na	0.001	0.000	0.000	0.000	0.000	0.000	0.003	0.000
K	0.000	0.000	0.000	0.000	0.000	0.000	0.000	0.000
Total	2.998	2.996	2.998	1.991	1.994	1.921	1.889	1.910
XFe^{3+}/Total Fe	0.667	0.667	0.667	1.000	1.000	1.000	1.000	1.000

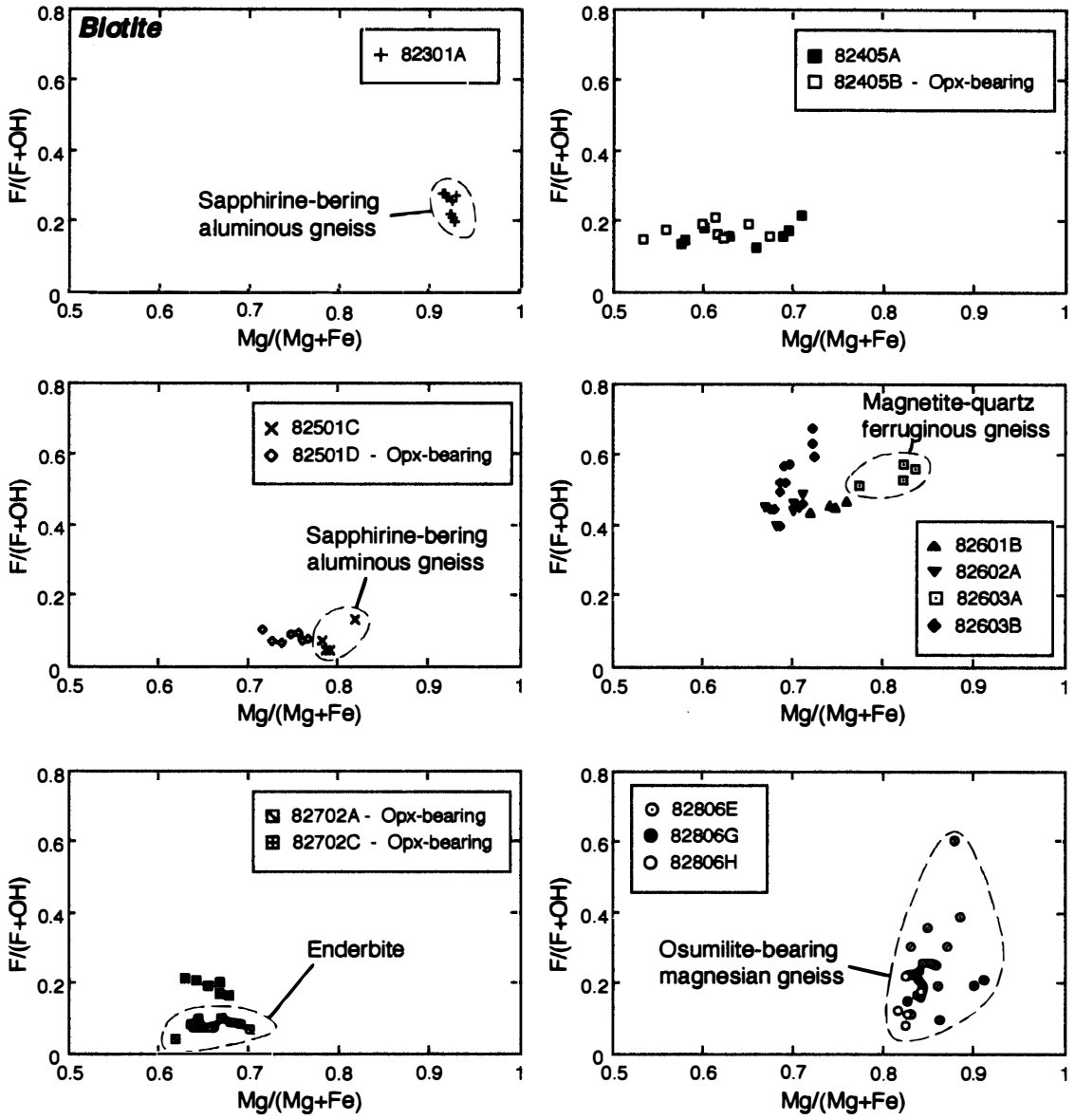

Fig. 7. Biotite chemical compositions in terms of Mg/(Mg+Fe) ratios and F/(F+OH) ratios. Each column represents samples from the same locality.

(sapphirine-bearing) and 2.4–3.9 wt% (osumilite-bearing) (Fig. 8a), but that from pelitic and ferruginous gneiss is commonly hercynite ($Mg/(Mg+Fe^{2+})$ ratios=0.13–0.38) with high ZnO content up to 13.7 wt%. Spinel, which is associated with opaque minerals, sometimes accompanies aluminiferous mineral (composed only of Al_2O_3=80–82 wt%), perhaps crysoberyl or aluminium hydrate.

4.4. Sapphirine

Sapphirine from aluminous gneiss show slightly Al-poorer than the ideal Si-Al substitution (Fig. 9a), which is considered to reflect ferric iron replacing Al. Fe^{3+}/total iron ratios are about 0.1–0.3 calculated from stoichiometry; $Mg/(Mg+Fe^{2+})$ ratios range

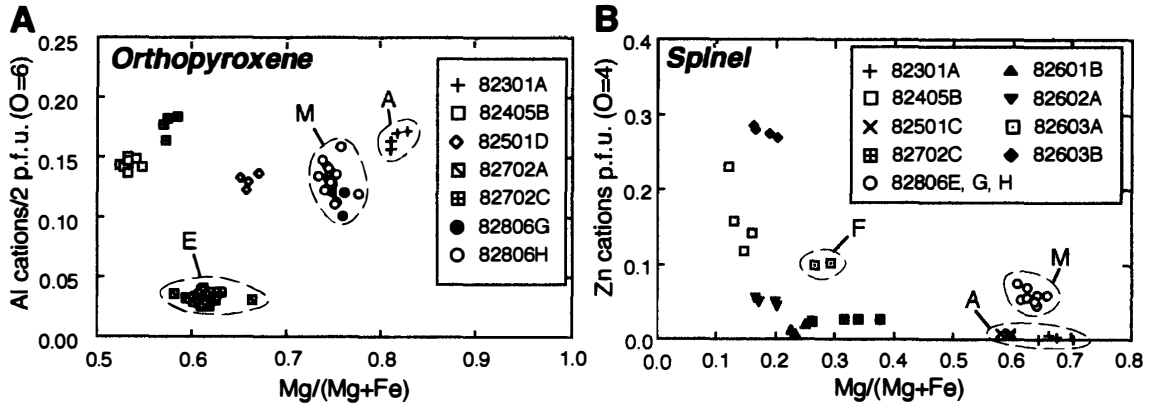

Fig. 8. (a) Orthopyroxene chemical compositions in terms of Mg/(Mg+Fe) ratios and Al cations. A: sapphirine-bearing aluminous gneiss. E: enderbite. M: osumilite-bearing magnesian gneiss. (b) Spinel chemical compositions in terms of Mg/(Mg+Fe) ratios and Zn cations. F: magnetite-quartz-bearing ferruginous gneiss.

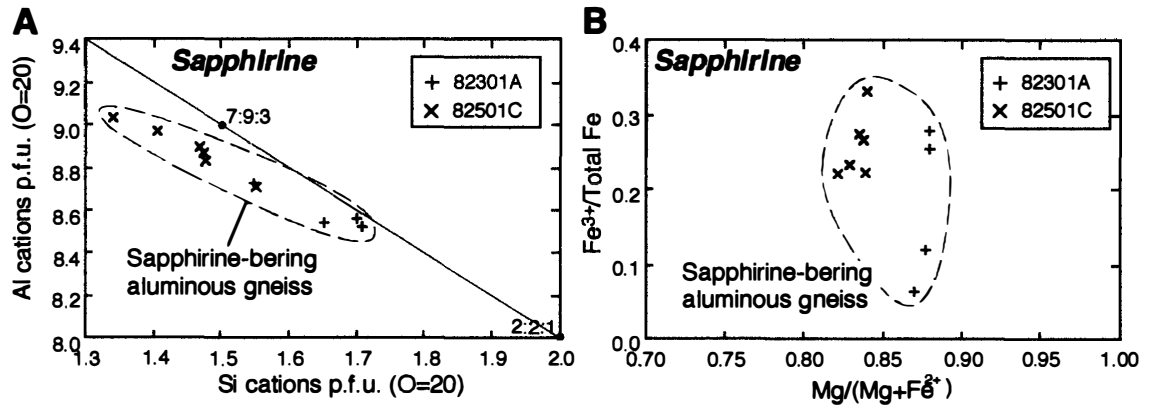

Fig. 9. (a) Sapphirine chemical compositions in terms of Si cations and Al cations. (b) Sapphirine chemical compositions in terms of Mg/(Mg+Fe) ratios and Fe^{3+}/total Fe ratios.

from 0.78 to 0.86 (Fig. 9b).

4.5. Garnet

A grossular-almandine-pyrope ternary plot for garnet is shown in Fig. 10. Both grossular and spessartine contents in garnet are less than 4 mol%. Compositional zoning of garnet is not obvious, but garnet surrounding magnetite shows weak compositional zoning of Fe decreasing and Mg and Ca increasing toward the rim. A thin garnet film rimming ilmenite, possibly retrograde product after ilmenite, shows significantly high almandine content, up to 68 mol%.

4.6. Cordierite

Cordierite represents the highest Mg/(Mg+Fe) phase among the constituent minerals. Mg/(Mg+Fe) ratios range from 0.78 to 0.80 in biotite-cordierite-garnet-orthopyroxene gneiss and from 0.89 to 0.94 in sapphirine and osumilite-bearing aluminous and

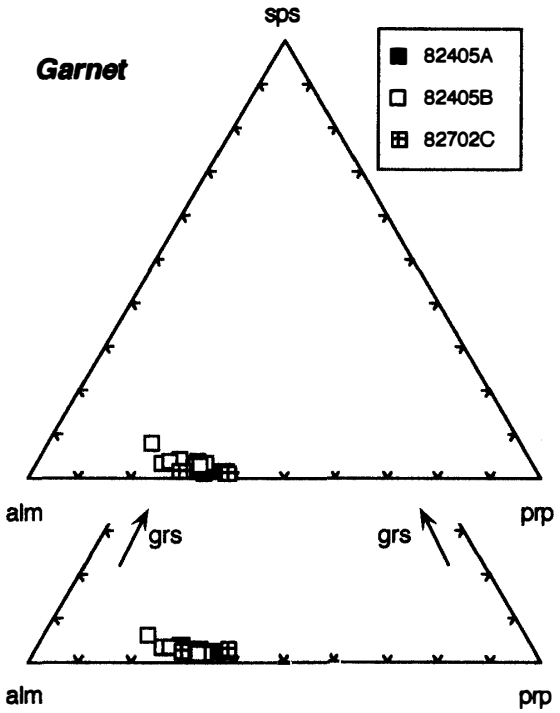

Fig. 10. Spessartine (sps) - almandine (alm) - pyrope (prp) and grossular (grs) - almandine (alm) - pyrope (prp) triangular plots of garnet.

magnesian gneisses. Cordierite in the study area has slightly hydrous (H_2O content = 0–1 wt%), judging from total wt% of analyses.

4.7. Osumilite

Osumilite, which is mostly replaced by fine-grained symplectite and survives only in sample 82806G, shows Mg/(Mg+Fe) ratios ranging from 0.87 to 0.90. Total wt% of analyses suggest that no volatile is included in the crystal.

4.8. Feldspars

Feldspars from a variety of metapelites show quite similar chemical compositions. Anorthite content in plagioclase ranges from 26 to 34 mol%, while albite content in K-feldspar is less than 21 mol% (Fig. 11), except that plagioclase in osumilite-bearing magnesian gneiss represents slightly higher anorthite content, 36–42 mol%. Plagioclase in enderbite shows markedly high anorthite contents up to 85 mol%.

5. Discussion

Orthopyroxene has high Al_2O_3 content ranging from 4.8 to 8.2 wt%, except orthopyroxene in enderbite (Al_2O_3 less than 2 wt%), which are similar values as reported for rocks in the study area (Waters, 1986; Nowicki *et al.*, 1995). Orthopyroxene commonly includes biotite as described above, suggesting that the orthopyroxene is formed through the breakdown of biotite. In many cases, orthopyroxene-bearing rocks lack K-feldspar; hence, the orthopyroxene is probably formed by dehydration melting:

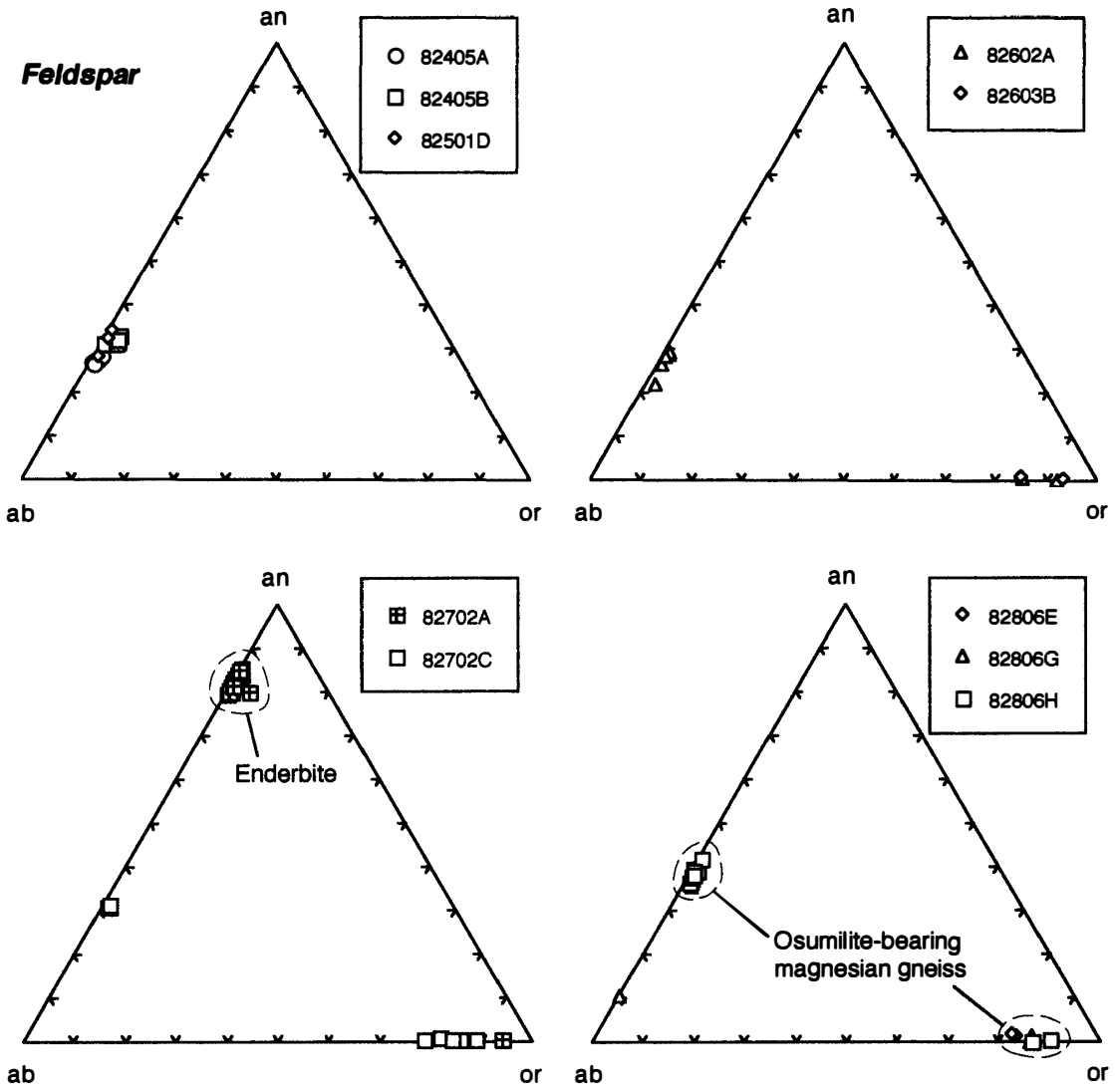

Fig. 11. Anorthite (an) - albite (ab) - orthoclase (or) triangular plots of feldspar.

$$\text{biotite} + \text{quartz} \rightarrow \text{orthopyroxene} + \text{melt},$$

rather than the solid-solid (dehydration) reaction:

$$\text{biotite} + \text{quartz} \rightarrow \text{orthopyroxene} + \text{K-feldspar}.$$

(Reaction equations are idealized for simplificity.)

Although there currently exists no direct textural evidence to constrain the orthopyroxene-forming reaction, dehydration melting of biotite is a plausible process to form orthopyroxene during granulite facies metamorphism. Experimental study implies that the biotite mineral chemistry, especially fluorine content, strongly affects the thermal stability of biotite; hence, the effect of fluorine is to extend biotite stability to higher temperature of dehydration melting of biotite to form orthopyroxene (Hensen and Osanai, 1994). However, in the studied samples, the presence of orthopyroxene has no

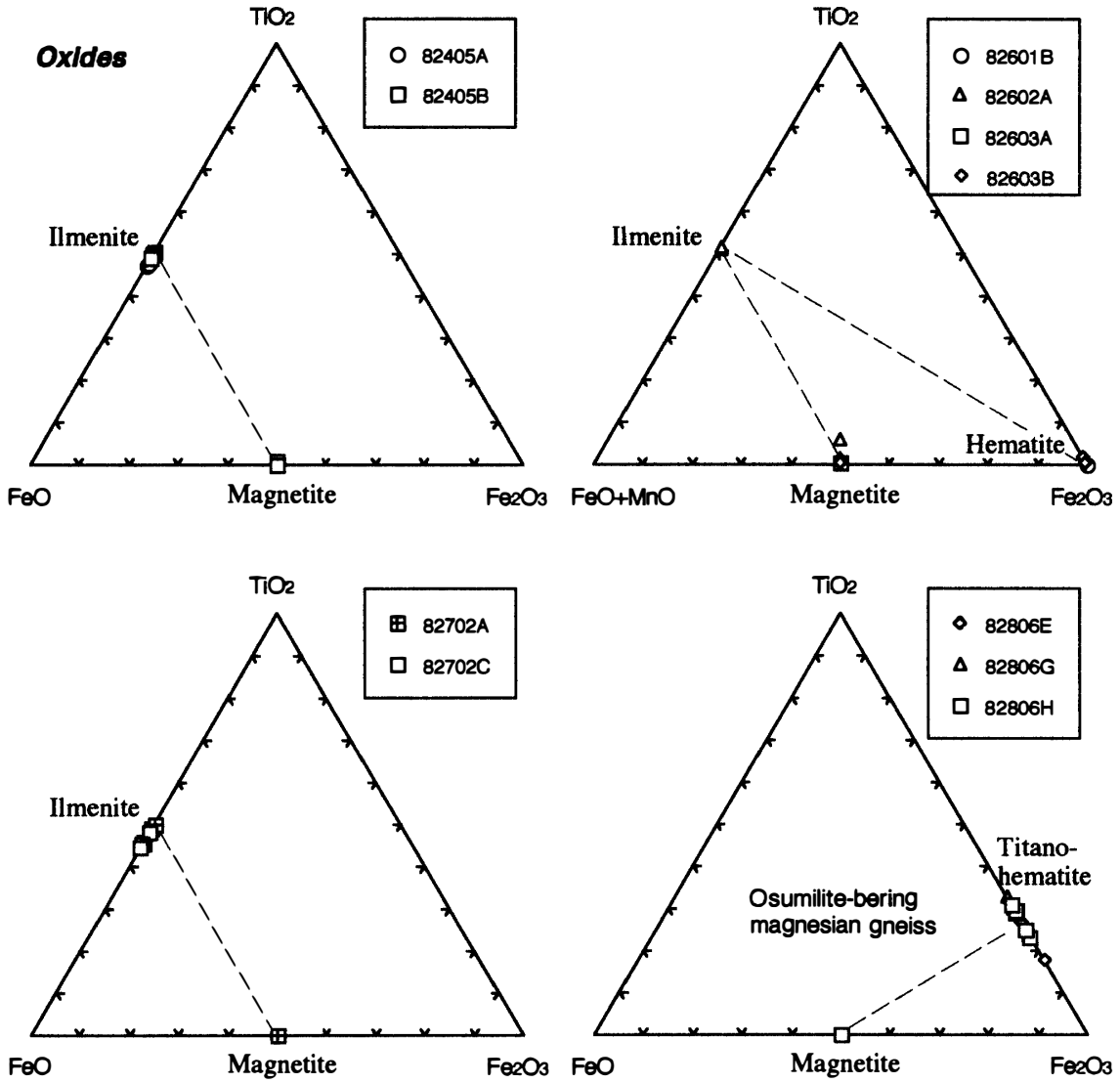

Fig. 12. TiO_2 - FeO - Fe_2O_3 triangular plots of opaque minerals.

correlation with the fluorine content of biotite (Fig. 7), and the formation of orthopyroxene needs an other cause, such as local decrease of water activity or the difference of bulk rock chemistry. Ougougdal and Robb (1996) reported both H_2O-rich and CO_2-rich fluid inclusions even in one sample from the study area, suggesting that the region is affected by diverse fluid populations. *P-T* conditions of the garnet-orthopyroxene equilibria in the garnet-orthopyroxene-biotite gneiss (405B) and the garnet-orthopyroxene-cordierite-biotite gneiss (702C) from the highest-grade (spinel-quartz) zone are estimated (820–870°C and 0.5 GPa, Fig. 13); they are comparable to those estimated by previous studies (Waters, 1988, 1991). In such *P-T* conditions, biotite dehydration melting to form orthopyroxene occurs in the case of lower X_{H_2O}. It is, therefore, probable that the formation of orthopyroxene was strongly affected by the decrease of H_2O activity on a local scale.

Spinel in Namaqualand contains a varying amount of ZnO, from 0.1 to 13.7 wt%.

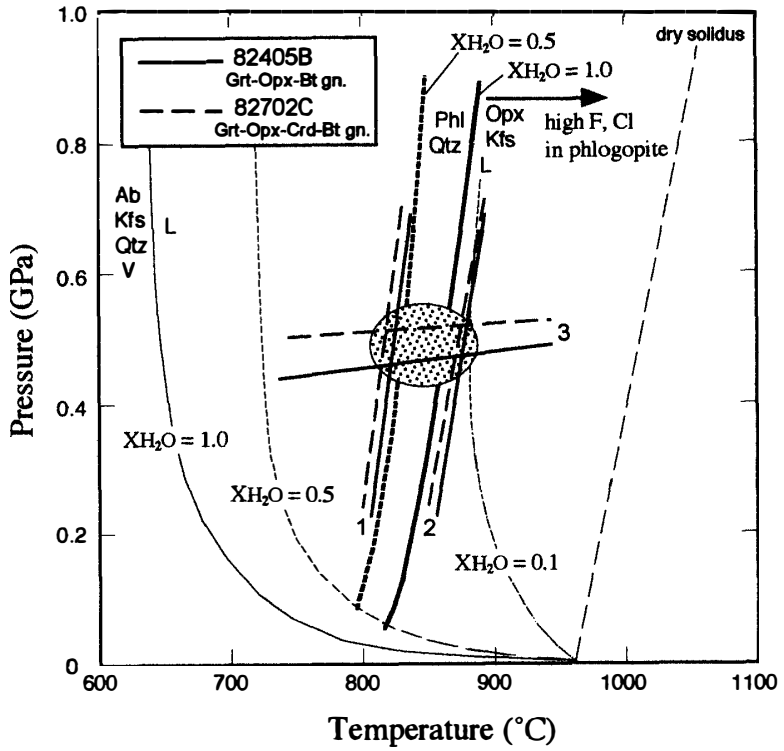

Fig. 13. P-T estimations for garnet-orthopyroxene equilibria in pelitic gneisses from the highest-grade (spinel-quartz) zone in Namaqualand. 1. Harley (1984). 2. Lee and Ganguly (1988). 3. Powell and Holland (1988). Melting curves for X_{H_2O} = 1.0, 0.5 and 0.1 are after Ebadi and Johannes (1991) and Newton (1990).

ZnO contents in spinel from sapphirine-bearing aluminous gneiss are low (<0.5 wt%) compared with other rock types. Those from osumilite-bearing magnesian gneiss are in the narrow compositional range of 2.4–3.9 wt%, whereas in the pelitic gneisses, spinel shows a narrow compositional range of ZnO content in each sample, but represents varying ZnO content depending on the sample even though the mineral assemblages are similar. These probably reflect the difference of bulk rock chemistry, but it is not certain whether these differences are originated from the protolith, or are caused by secondary processes, such as metasomatism or melting. The formation of Zn-poor Fe-Mg spinel in Namaqualand was discussed by Waters (1991). He concluded that some of the spinel coexisting with quartz was formed from cordierite. He also suggested that the magnetite and ilmenite associated with spinel are formed as oxidation exsolution products after high titaniferous and ferric iron-rich spinel. However, spinel associated with ilmenite, hematite and magnetite in this study is relatively fine-grained and occurs commonly at the rim of the opaque minerals. These textural relationships are in the opposite sense to those reported by Waters (1991) and rather imply that the spinel is produced after aluminiferous iron (-titan) oxides.

Acknowledgments

Dr. Y. Osanai and Prof. M. Arima are acknowledged for their critical reading of the manuscript. This study was supported by a Grant-in-Aid for Scientific Research from the Japanese Ministry of Education, Science, Sports and Culture to K. Shiraishi (No. 09041116).

References

Clifford, T.N., Barton, E.S., Retief, E.A., Rex, D.C. and Fanning, C.M. (1995): A crustal progenitor for the intrusive anorthosite-charnockite kindred of the cupriferous Koperberg Suite, O'okiep District, Namaqualand, South Africa; new isotope data for the country rocks and the intrusives. J. Petrol., **36**, 231–258.

Ebadi, A. and Johannes, W. (1991): Beginning of melting and composition of first melts in the system Qz-Ab-Or-H_2O-CO_2. Contrib. Mineral. Petrol., **106**, 286–295.

Harley, S.L. (1984): An experimental study of the partitioning of Fe and Mg between garnet and orthopyroxene. Contrib. Mineral. Petrol., **86**, 359–373.

Hensen, B.J. and Osanai, Y. (1994): Experimental study of dehydration melting of F-bearing biotite in model pelitic compositions. Mineral. Mag., **58A**, 410–411.

Hiroi, Y., Hokada, T., Motoyoshi, Y., Shimura, T., Yuhara, M., Shiraishi, K., Grantham, G.H. and Knoper, M.W. (2001): New evidence for prograde metamorphism and partial melting of Mg-Al-rich granulites from western Namaqualand, South Africa. Mem. Natl Inst. Polar Res., Spec. Issue, **55**, 87–104.

Lee, H.Y. and Ganguly, J. (1988): Equilibrium compositions of coexisting garnet and orthopyroxene: experimental determinations in the system FeO-MgO-Al_2O_3-SiO_2, and applications. J. Petrol., **29**, 93–113.

Moore, J.M., Waters, D.J. and Niven, M.L. (1990): Werdingite, a new boronsilicate mineral from the granulite facies of the western Namaqualand metamorphic complex, South Africa. Am. Mineral., **75**, 415–420.

Newton, R.C. (1990): Fluids and melting in the Archaean deep crust of southern India. High-temperature Metamorphism and Crustal Anatexis, ed. by J.R. Ashworth and M. Brown. London, Unwin Hyman, 149–179.

Nowicki, T.E., Frimmel, H.E. and Waters, D.J. (1995): The occurrence of osumilite in pelitic granulites of the Namaqualand Metamorphic Complex, South Africa. S. Afr. J. Geol., **98**, 191–201.

Ougougdal, M.A. and Robb, L.J. (1996): The nature of fluids associated with granulite facies metamorphism in the Okiep Copper District, Namaqualand, South Africa. S. Afr. J. Geol., **99**, 197–208.

Powell, R. and Holland, T.J.B. (1988): An internally consistent thermodynamic dataset with uncertainties and correlations: 3. Applications to geobarometry, worked examples and a computer program. J. Metamorph. Geol., **6**, 173–204.

Raith, J.G. and Harley, S.L. (1998): Low-P/high-T metamorphism in the Okiep Copper District, western Namaqualand, South Africa. J. Metamorph. Geol., **16**, 281–305.

Robb, L.J., Armstrong, R.A. and Waters, D.J. (1999): The history of granulite-facies metamorphism and crustal growth from single zircon U-Pb geochronology: Namaqualand, South Africa. J. Petrol., **40**, 1747–1770.

Spear, F. (1993): Metamorphic Phase Equilibria and Pressure-Temperature-Time Paths. Washington, D.C., Mineralogical Society of America, 799 p.

Waters, D.J. (1986): Metamorphic history of sapphirine-bearing and related gneisses from Namaqualand, South Africa. J. Petrol., **27**, 541–565.

Waters, D.J. (1988): Partial melting and the formation of granulite facies assemblages in Namaqualand, South Africa. J. Metamorph. Geol., **6**, 378–404.

Waters, D.J. (1989): Metamorphic evidence for the heating and cooling path of Namaqualand granulites. Evolution of Metamorphic Belts, ed. by J.S. Daly *et al.* Oxford, Blackwell Sci. Publ., 357–363.

Waters, D.J. (1990): Thermal history and tectonic setting of the Namaqualand granulites, southern Africa: clues to Proterozoic crustal development. Granulites and Crustal Evolution, ed. by D. Vielzeuf and P. Vidal. Netherlands, Kluwer Academic Publ., 243–256.

Waters, D.J. (1991): Hercynite-quartz granulites: phase relations, and implications for crustal processes. Eur. J. Mineral., **3**, 367–386.

Waters, D.J. and Moore, J.M. (1985): Konerupine in Mg-Al-rich gneisses from Namaqualand, South Africa: mineralogy and evidence for late-metamorphic fluid activity. Contrib. Mineral. Petrol., **91**, 369–382.

Waters, D.J. and Whales, C.J. (1984): Dehydration melting and the granulite transition in metapelites from southern Namaqualand, S. Africa. Contrib. Mineral. Petrol., **88**, 269–275.

(Received December 14, 2000; Revised manuscript accepted July 27, 2001)